

DENSE RANGE IMAGE SMOOTHING USING ADAPTIVE REGULARIZATION

Yiyong Sun[†], Joon-Ki Paik[‡], Jeffery R. Price[†], Mongi A. Abidi[†]

[†]Imaging, Robotics and Intelligent Systems Laboratory,

Department of Electrical and Computer Engineering, The University of Tennessee, Knoxville

[‡]Department of Image Engineering, Graduate School of Advanced Imaging Science,
Chung-Ang University, Seoul, Korea

ABSTRACT

We propose an adaptive regularization algorithm for smoothing dense range images using a novel, first order stabilizing function. The stabilizer we suggest is based upon minimizing the reconstructed surface area and is derived in the native, spherical coordinate system of the range scanner. This allows adjustments to be made along only the direction of measurement, thereby preventing the data overlapping problem that can arise in dense images. Adaptation is achieved by adjusting the regularization parameter according to the results of 2D edge analysis. Results indicate effective noise suppression along with well preserved edges and details in the reconstructed, 3D surfaces.

I. INTRODUCTION

In this paper, we propose a regularization method for smoothing dense range images while preserving the edges. Laser range scanners are widely used in 3D reconstruction, but the range measurements are corrupted by many different sources of noise [1] and often need to be preprocessed before further use. Since many dense range image preprocessing approaches are mainly based on the 2D nature, the valuable 3D surface information is not fully exploited.

For sparse range images, regularization methods are often used for 3D reconstruction. Since there is not enough data to detect discontinuities in sparse range images, edges are preserved through the application of a penalty energy term in the reconstruction. This penalty term generally makes minimization of the total energy function very difficult. Unlike the sparse case, discontinuities can be predetermined by edge analysis when we apply regularization for dense image smoothing.

In dense range image reconstruction, we can no longer regard the surface as a graph as is done in many sparse image applications. Here, we obtain the stabilizing function in a spherical coordinate system common to some laser range scanners. (Specifically, we use a Perceptron scanner). In this coordinate system, we can optimally adjust the range data along only the direction of the measurement.

In this paper, we examine the first order stabilizing

functions for use in the regularization. The first order stabilizer discussed here relates to the reconstructed surface area. By minimizing the reconstructed surface area, a smoother surface is produced. Since the stabilizing term will be the square root of a function that makes minimization difficult if we directly minimize the surface area, we use an alternative stabilizing term and its validity is shown. The smoothing factor, or the regularization parameter, is adaptively determined by edge analysis.

Experimental results show that the proposed first order, surface area based regularization method significantly improves range image smoothness, while preserving data consistency, especially along the edges.

II. MINIMAL SURFACE STABILIZER

Invariant reconstruction of surfaces by regularization has been previously studied in [2,3,4,5]. Most of the techniques are used for surface recovery from sparse data, which is essentially an interpolation problem. Reconstruction from a single-view, dense range image, however, is a smoothing or restoration problem. In many applications, such as mesh simplification and/or segmentation, the dense 3D data will be reduced [6]. The performance of such applications depends strongly on the accuracy of the range data. Traditionally, raw images are preprocessed using some filtering method, where there is no control of the data faithfulness and the information about the surface is not properly used. With the regularization method, we can control the tradeoff between smoothness and data compatibility with an appropriate stabilizing term related to the 3D surface properties.

Traditionally, the surface is considered as a graph $z(x, y)$ and represented as z_{ij} over a rectangular grid. Letting c_{ij} represent the observed data, the total energy can be written as

$$E(z) = \sum_{ij} (z_{ij} - c_{ij})^2 / \sigma_{ij}^2 + \lambda F_s$$

where $1/\sigma_{ij}$ denotes the confidence of the measurement. In practice, $1/\sigma_{ij}$ is approximated by the surface slant, $\cos \phi$, with respect to the incident laser. The larger the angle ϕ between the surface normal and the direction of measurement, the smaller the confidence is. Because $(z_{ij} - c_{ij})/\sigma_{ij}$ represents the perpendicular distance

between the estimated and real surfaces, it is viewpoint invariant. The stabilizing function F_s can take different forms. For example, first order regularization is used in [2] while a second order model is investigated in [4].

Estimating z_{ij} is feasible for sparse data. But in dense range images from a range scanner with a spherical system, $z(x, y)$ is not necessarily a graph. Therefore, we would instead like to estimate the range r_{ij} so that all refinement takes place along the line of measurement. If we estimate z_{ij} in a dense range image, the refinement might cause some surface measurements to be hidden behind others.

For the Perceptron range scanner we use, each pixel in the range image R_{ij} is converted to Cartesian coordinates (x_{ij}, y_{ij}, z_{ij}) as follows:

$$\begin{aligned} x_{ij} &= dx + r \sin \alpha \\ y_{ij} &= dy + r \cos \alpha \sin \beta \end{aligned} \quad (1)$$

$$\begin{aligned} z_{ij} &= dz - r \cos \alpha \cos \beta \\ \alpha &= \alpha_0 + H(\text{col} / 2 - j) / \text{col} \\ \beta &= \beta_0 + V(\text{row} / 2 - i) / \text{row} \end{aligned} \quad (2)$$

$$\begin{aligned} r_1 &= (dz - h_2) / \delta \\ r_2 &= \sqrt{dx^2 + (h_2 + dy)^2} / \delta \\ r &= (R_{ij} + r_0 - r_1 - r_2) / \delta \end{aligned} \quad (3)$$

$$\begin{aligned} dx &= (h_2 + dy) \tan \alpha \\ dy &= dz \tan(\theta + 0.5\beta) \end{aligned} \quad (4)$$

$$dz = -h_1(1.0 - \cos \alpha) / \tan \gamma$$

where $h_1, h_2, \gamma, \theta, \alpha_0, \beta_0, H, V, r_0, \delta$ are the calibration parameters of the scanner, and row, col refer to the image size.

To estimate r , we use the parameterization as

$$X(\alpha, \beta) = (r \sin \alpha, r \cos \alpha \sin \beta, -r \cos \alpha \cos \beta) \quad (5)$$

and we ignore small dx, dy, dz in the analysis.

The coefficients of the first fundamental form [7] in the basis of $\{X_\alpha, X_\beta\}$ are

$$\begin{aligned} E &= r^2 + r_\alpha^2 \\ F &= r_\alpha r_\beta \\ G &= r^2 \cos^2 \alpha + r_\beta^2 \end{aligned} \quad (6)$$

We denote c as the observed value of r . So the energy function can be written as

$$E(r) = \sum_{ij} (r_{ij} - c_{ij})^2 / \sigma_{ij}^2 + F_s \quad (7)$$

We let the stabilizing function F_s be the surface area. Minimizing F_s will give a minimal surface whose mean curvature is zero. Generally, minimizing surface area will give a smooth surface, though the minimal surface is not necessarily smooth [8].

The surface area is calculated as

$$F_s = A = \int_D \sqrt{EG - F^2} d\alpha d\beta \quad (8)$$

where D is the domain of (α, β) . As (8) is not easily minimized because of the square root operation, we instead minimize

$$F_s = \int_D (EG - F^2) d\alpha d\beta \quad (9)$$

The validity of doing this can be proven as follows. First we define

$$\begin{aligned} \xi_{iN+j} &= \sqrt{E_{ij} G_{ij} - F_{ij}^2} \\ \eta_{iN+j} &= 1 \end{aligned}$$

for $i < M, j < N$, and

$$\xi_k = 0, \eta_k = 0$$

for $k > MN$. Then, by the Cauchy-Schwarz inequality, we know that

$$\sum_{j=1}^{\infty} |\xi_j \eta_j| \leq \sqrt{\sum_{k=1}^{\infty} |\xi_k|^2} \sqrt{\sum_{m=1}^{\infty} |\eta_m|^2},$$

where $\sum_{j=1}^{\infty} |\xi_j|^2 < \infty$ and $\sum_{j=1}^{\infty} |\eta_j|^2 < \infty$ as only finite number of terms are nonzero. This then yields

$$\sum_{i,j}^{M,N} \sqrt{E_{ij} G_{ij} - F_{ij}^2} \leq \sqrt{MN \sum_{i,j}^{M,N} (E_{ij} G_{ij} - F_{ij}^2)},$$

which shows that the convergence of (9) implies the convergence of (8). Therefore from (6), (7) and (9), the total energy is given by

$$\begin{aligned} E(r) &= \sum_{ij} (r_{ij} - c_{ij})^2 / \sigma_{ij}^2 + \\ &\lambda_{ij} \sum_{ij} (r_{ij}^4 \cos^2 \alpha + r_{ij}^2 r_\beta^2 + r_\alpha^2 r_{ij}^2 \cos^2 \alpha) \end{aligned} \quad (10)$$

where r_α and r_β can be approximated using forward finite differences. Although there are many methods to attempt minimization of (10), we use a simple gradient descent. The estimation r'_{ij} of every measurement r_{ij} is as follows.

$$\begin{aligned} r'_{ij} &= 2(r_{ij} - c_{ij}) + \lambda_{ij} \{ 4r_{ij}^3 \cos^2 \alpha \\ &+ [2r_{ij} (r_{i,j+1} - r_{ij})^2 - 2r_{ij}^2 (r_{i,j+1} - r_{ij}) + 2r_{i,j-1} (r_{ij} - r_{i,j-1})] \left(\frac{\cos \alpha}{d\alpha} \right)^2 \\ &+ [2r_{ij} (r_{i+1,j} - r_{ij})^2 - 2r_{ij}^2 (r_{i+1,j} - r_{ij}) + 2r_{i-1,j} (r_{ij} - r_{i-1,j})] \left(\frac{1}{d\beta} \right) \} \end{aligned} \quad (11)$$

III. EDGE PRESERVATION

Incorporation of the regularizing term in energy, as shown in (10), tends to suppress local change in the range image. Although the smoothing function is good for suppressing undesired noise, it also degrades important features such as edges, corners, and segment boundaries. Using an additional energy term to preserve discontinuity, however, makes the minimization very difficult in general. Instead, we use the results of 2D edge analysis to adaptively weight the smoothing factor λ so that edges are preserved during the regularization.

Although there are various simple edge enhancement

filters, we use the optimal edge enhancer [9], which guarantees both good detection and localization. Let g_{ij} represent the (i, j) -th pixel of Gaussian filtered version of r_{ij} , and let $J_x(i, j)$ and $J_y(i, j)$ be the gradient component of g_{ij} in the horizontal and vertical directions, respectively. Then the optimal edge strength image can be obtained as

$$e_s(i, j) = \sqrt{J_x^2(i, j) + J_y^2(i, j)}. \quad (12)$$

The regularizing term in (10) can adaptively be weighted as in [10] using

$$\lambda_{ij} = \frac{k}{1 + \theta e_s^2(i, j)}, \quad (13)$$

where θ , $0 < \theta < 1$, represents a parameter that determines sensitivity of edge strength, and k is a scaling parameter.

The selection of k generally depends on the desired data compatibility as well as the level of noise reduction. Since the stabilizing term in the energy function has a much larger scale than the data compatibility term, k is very small in our application. Here we introduce a method to approximately estimate k . We determine a k so that the average relative adjustment (ARA) from the observed range value is in the same range as that produced by other popular techniques, such as median filtering, which we employ in our experiments. For one example image, the ARA was found to be 0.44% after applying 3×3 median filtering twice. We select k to make the ARA smaller than median filtering method. For example, the ARA was found to be 0.25% after 50 iterations using the regularization method for the same image. In experiments we found that the regularization method does not suppress impulsive (salt and pepper) noise effectively. We therefore apply median filtering twice, prior to regularization. For the example image we have been discussing, the ARA was found to be 0.50% after median filtering twice and 50 iterations of regularization. This is comparable to the ARA produced using only median filtering.

IV. EXPERIMENTAL RESULTS

Experimental results from minimizing (10) are shown here. Fig. 1 shows the raw, unprocessed data and Fig. 2 shows the corresponding, non-adaptive regularization results. The median filtered result, the edge map, and both non-adaptive and adaptive regularization results are shown in Fig. 3. Note in Fig. 3 the wires on the cubicle wall behind the monitor that are preserved by the adaptive regularization.

Equation (11) is obtained by approximating r_α and r_β using

$$r_\alpha = \frac{1}{d\alpha} (r_{i,j+1} - r_{ij}) \quad \text{and} \quad r_\beta = \frac{1}{d\beta} (r_{i+1,j} - r_{ij}). \quad (14)$$

If we instead use three point polynomial interpolation to

estimate r_α and r_β , such as,

$$r_\alpha = \frac{1}{2d\alpha} (r_{i,j+1} - r_{i,j-1}) \quad \text{and} \quad r_\beta = \frac{1}{2d\beta} (r_{i+1,j} - r_{i-1,j}), \quad (15)$$

we will have an estimation formula:

$$\begin{aligned} r'_{ij} = & 2(r_{ij} - c_{ij}) + \lambda_{ij} \{ 4r_{ij}^3 \cos^2 \alpha \\ & + [2r_{ij}(r_{i,j+1} - r_{i,j-1})^2 - 2r_{i,j+1}^2(r_{i,j+2} - r_{ij}) + 2r_{i,j-1}^2(r_{ij} - r_{i,j-2})] \left(\frac{\cos \alpha}{2d\alpha} \right)^2 \\ & + [2r_{ij}(r_{i+1,j} - r_{i-1,j})^2 - 2r_{i+1,j}^2(r_{i+2,j} - r_{ij}) + 2r_{i-1,j}^2(r_{ij} - r_{i-2,j})] \left(\frac{1}{2d\beta} \right)^2 \} \end{aligned} \quad (16)$$

In our experiments, (15) makes the minimization more robust and k can be set large to speed up the convergence. One iteration using (16) achieves almost the same smoothing result as the 50 iterations using (11). Fast convergence makes the algorithm more attractive in real world applications.

ACKNOWLEDGEMENTS

The research was supported by the U.S. Department of Energy's University Research Program in Robotics (Universities of Florida, Michigan, New Mexico, Tennessee, and Texas), grant DOE-DE-FG02-86NE37968.

REFERENCES

- [1] R. Pito, "Characterization, calibration, and use of the Perceptron laser range finder in a controlled environment," *Technical Report MS-CIS-95-05*, Univ. of Pennsylvania GRASP Laboratory, Philadelphia, PA, January 1995.
- [2] June H. Yi and David M. Chelberg, "Discontinuity-preserving and viewpoint invariant reconstruction of visible surface using a first order regularization," *IEEE Trans. PAMI*, vol. 17, no. 6, pp. 624-629, June 1995.
- [3] A. Blake and A. Zisserman, *Visual reconstruction*, Cambridge, Mass.: MIT Press, 1987.
- [4] R.L. Stevenson and E.J. Delp, "Viewpoint invariant recovery of visual surface from sparse data," *IEEE Trans. PAMI*, vol. 14, no. 9, pp. 897-909, September 1992.
- [5] Nutin M. Vaidya and Kim L. Boyer, "Discontinuity-preserving surface reconstruction using stochastic differential equations," *Computer Vision and Image Understanding*, vol. 72, no. 3, pp. 257-270, December 1998.
- [6] C. S. Gourley, C. Dumont, and M. A. Abidi, "Pattern vector based reduction of 3D meshes created from multimodal data sets," in *Proceedings of SPIE AeroSense '99: Aerospace/Defense Sensing and Controls*, vol. 3693, pp. 112-123, Orlando, FL, April 1999.
- [7] Manfredo P. Do Carmo, *Differential geometry of curves and surfaces*, Prentice Hall, 1976.
- [8] R. T. Whitaker, "A Level-Set Approach to 3D Reconstruction From Range Data," *International Journal of Computer Vision*, vol. 29, no. 3, October 1998.
- [9] J. Canny, "A computational approach to edge detection," *IEEE Trans. PAMI*, vol. 8, pp. 679-698, 1986.
- [10] A. K. Katsaggelos, "Iterative image restoration algorithms," *Optical Engineering*, vol. 28, no. 7, pp. 735-748, 1989.

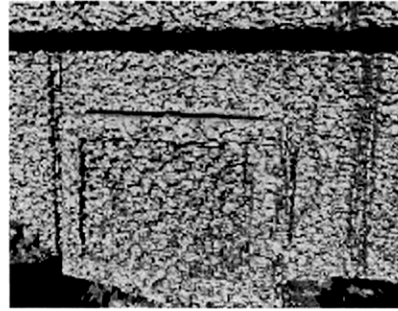
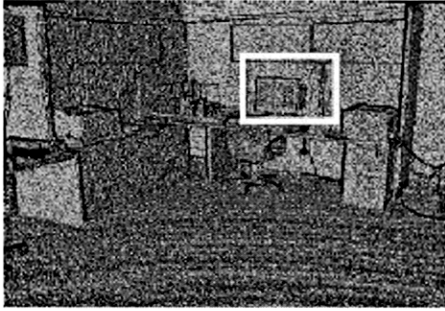


Fig. 1: Raw image (left) and zoomed portion (right).

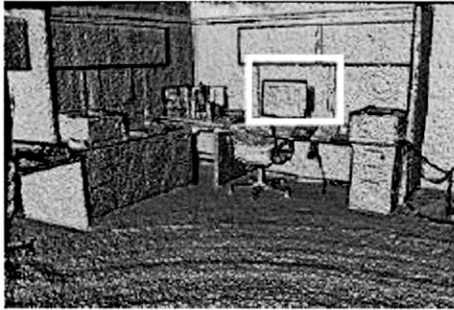


Fig. 2: Regularization result (left) and zoomed portion (right).

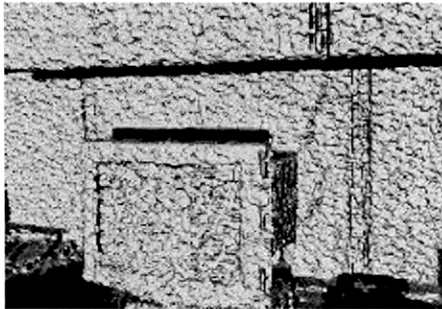


Fig. 3: Median filtered result (top left), edge map (top right), non-adaptive regularization result (bottom left), and adaptive regularization result (bottom right).